Synthesis and Optical Characterization of Annatto (Bixa orellana L.)-Doped PVDF Samples: Ultraviolet Optical Absorption Enhancement and Bandgap Decrease

E.A. Falcao*, T.S. Silva, L.G.N. Muniz, and E.S.S. Rodrigues

Post-Graduation Program in Environmental Science and Technology (PPGCTA), Federal University of Grande Dourados (UFGD), Rodovia Dourados-Itahum, km 12, Dourados, MS, Zip: 79.804-970, Brazil

Abstract: In this work, samples of PVDF/Annatto (PVDF/An) were synthesized and characterized as a function of annatto concentration. The FT-IR results show the incorporation of An in the polymeric matrix, without changing the relative percentage of the β phase. The UV optical properties were studied by the UV-Vis technique. The addition of An to PVDF changes the optical absorption in the UV region from 200 nm to 650 nm. The optical transmittance decreases from 60% for PVDF/An 0% to 0% for PVDF/An 5% at 540 nm. The optical absorption edge is redshifted from 251 nm to 645 nm, and the width at half weight increases approximately 1083 %, reaching 355 nm. For doped samples, the extinction coefficient presents two peaks at 470 nm and 499 nm, which might be associated with bixin. Skin depth results show a 64% decrease in $E_{cut\text{-}off}$ from 6.18 eV to 2.50 eV. The addition of An shifts the optical bandgap toward lowest energies. Urbach energy decreases as An content increases. This result is consistent with the results observed for the absorption edge and the optical bandgap. Finally, the obtained results show that PVDF/An samples are potential candidates for optical and photonic applications.

Keywords: PVDF, Bixa orellana L., Optical bandgap, Ferroelectric polymer, UV absorption.

INTRODUCTION

Poly(vinylidene fluoride), PVDF, is a semi-crystalline polymer of great interest in studies involving films and composites, primarily due to its polymorphism and the sensitivity of its structure to processing conditions. PVDF can crystallize in five crystalline phases: α, β, γ, δ, and ε. However, most studies focus on α and β phase due to their enhanced mechanical and ferroelectric properties. Nevertheless, the proportions of the α, β, and γ crystalline phases may vary depending on the solvent used, solvent evaporation, thermal history, and the presence of incorporated components in the polymeric matrix [1, 2]. The β phase is associated with the all-trans conformation of polymeric chains and the alignment of electrical dipoles related to C–F bonds. For this reason, the β phase is related to piezoelectric, ferroelectric, and dielectric properties of the PVDF matrix [1, 2]. The β phase is the most studied for electro-electronic applications. The addition of different fillers can improve piezoelectric and ferroelectric properties and also improve the optical properties of the PVDF matrix. Among these improvements, it can be cited enhancement of UV optical absorption, optical fluorescence, and optical bandgap change, associated with structural disorder [3-6]. In this sense, PVDF can be treated as a functional matrix whose response depends on its crystalline structure and the chemical nature of the incorporated material. In previous research, UV-Vis techniques have been used to study the optical properties of PVDF/Nd_2O_3, including the optical absorption coefficient, extinction coefficient, skin depth, and Urbach energy. This study shows that the dopant addition changes the interaction between the doped material and electromagnetic radiation [3]. Similar studies have been performed in other systems, such as neodymium compounds, organic complexes, and natural fillers, in which the optical response of PVDF becomes dependent on the interaction between the polymer and the incorporated component [4-6].

In this context, annatto (*Bixa orellana* L.) is a natural colorant from yellow to orange and flavoring agent. The principal interest in this natural material is due to the presence of pigments in its seeds, derived from norbixin, bixin, along with methyl bixin, β-carotene, lutein, cryptoxanthin, and zeaxanthin [7]. In annatto, bixin is the majority carotenoid present. In contrast, norbixin is primarily associated with the transformation of bixin in an alkaline medium, which alters the pigment's polarity and affinity for the medium [8-11]. These compounds present conjugated systems that favor electronic transitions in the visible region of the electromagnetic spectrum, which explain the characteristic color of materials derived from annatto [11, 12]. All these characteristics make annatto an interesting filler for polymer materials. In the literature, different studies report the incorporation of annatto-derived materials into polymeric matrices, such as PMMA, PANI and PHB [13-15]. In another study, norbixin extracted from annatto was used to produce conductive composites for electrochemical sensors

*Address correspondence to this author at the Federal University of Grande Dourados (UFGD), Rodovia Dourados-Itahum, km 12, Dourados, ZIP code 79.804-970, MS, Brazil;
E-mail: evaristofalcao@ufgd.edu.br; https://orcid.org/0000-0002-3778-1723

Received on 09-07-2026 Accepted on 19-08-2026 Published on 24-08-2026

E-ISSN: 2311-8717/26

and to promote bone tissue repair [15]. These studies show that annatto-derived materials can be used for optical and technological applications. Therefore, the objective of this work was to synthesize and characterize the optical properties of PVDF samples doped with annatto (An) or (PVDF/An) as a function of An concentration via the UV-Vis technique.

MATERIALS AND METHODS

PVDF powder was donated by Arkema of Brazil (Kynar™) without pooling or purification. Dimethylformamide (DMF) (99.8% purity) from Vetec™ was used as the solvent. The seeds of Bixa orellana L. were harvested from the annatto tree and used as the source of the natural dopant incorporated into the PVDF matrix. Annatto seeds were dried in an oven at 50 °C for 168 h. Subsequently, the dried material was ground using a Britânia™ BMX400P knife mill and, later, a zirconia microbead mill. Following this step, the resulting powder was sieved through a 0.250 mm (60 mesh) screen, yielding an annatto powder with controlled particle size. To prepare the pure PVDF sample, 120 mg of the polymer powder was dissolved in DMF at room temperature. For the PVDF/An composites, the An loadings were 1%, 2%, 3%, 4%, and 5% by mass relative to PVDF. The PVDF and An powders were dissolved separately in DMF at room temperature. Subsequently, the PVDF and An solutions were mixed, stirred, and poured into glass Petri dishes according to the proportions established for each composition. Finally, the samples were oven-dried at 50 °C for 16 h to remove the solvent and form the films. The obtained samples were identified as PVDF/An 0% (pure PVDF), PVDF/An 1%, PVDF/An 2%, PVDF/An 3%, PVDF/An 4%, and PVDF/An 5%, respectively. FT-IR/ATR measurements were performed using a Bruker Invenio R spectrometer, equipped with a diamond ATR unit. The scan was performed over 4000–100 cm^{-1} with 64 scans at a resolution of 1 cm^{-1}. Background spectra were automatically recorded and subtracted, and the resulting spectra were saved in OPUS software. The UV-Vis measurements were performed using a Shimadzu spectrophotometer model UV-2700i with diffuse reflectance in the wavelength range of 200–1400 nm, and the LabSolutions acquisition program provided diffuse transmittance and absorbance results.

RESULTS AND DISCUSSIONS

The obtained samples presented thicknesses of 0,050 ± 0,007 mm, 0,052 ± 0,008 mm, 0,056 ± 0,005 mm, 0,062 ± 0,004 mm, 0,066 ± 0,005 mm e 0,074 ± 0,005 mm for PVDF/An 0%, PVDF/An 1%, PVDF/An 2%, PVDF/An 3%, PVDF/An 4%, and PVDF/An 5% respectively. These results are the average of measurements taken at six points on the sample.

The FTIR spectrum of the PVDF/An films, shown in Figure **1**, exhibited vibrational bands characteristic of the polymer matrix, consistent with different crystalline phases of PVDF. For PVDF/An 0%, it is possible to observe the typical absorption peaks of α-phase at 1424, 1381, 1212, 975, 855, 795, 763, 615, and 530 cm^{-1}. For β-phase, the peaks were found at 1275−1279, 840, and 511 cm^{-1}, and for γ-phase at 1234, 834, 812, 778, and 484 cm^{-1} [1,4]. PVDF exhibits a peak at 1401 cm^{-1} which is associated with CH_2 wagging mode [16]. For doped samples, the contribution of annatto to the composite must be interpreted in light of the preparation method employed. Since the material used consisted of dried, ground, and sieved *Bixa orellana* L. seeds. Thus, the powder incorporated into the film represents a complex plant matrix rich in annatto

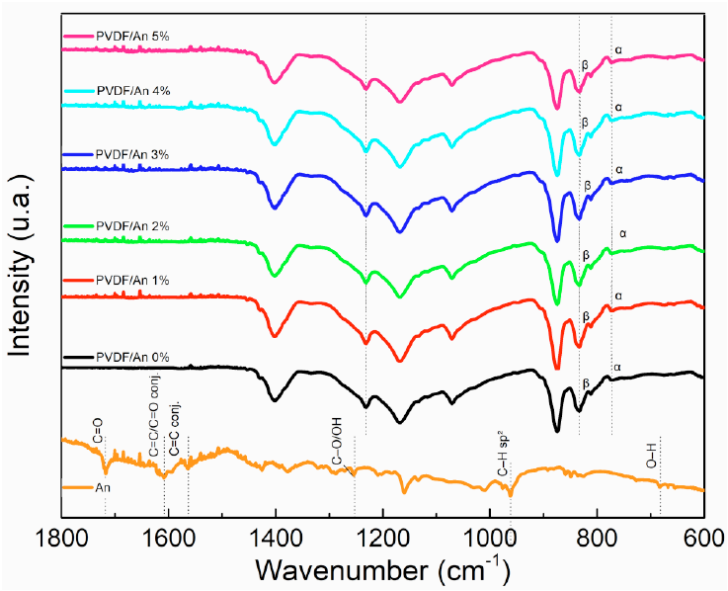

Figure 1: Measurements of FT-IR/ATR for PVDF/An as a function of An concentration.

constituents, particularly compounds associated with carotenoids such as bixin [7-12]. In this context, the region between 1713 and 1717 cm^{-1} is particularly significant, as it corresponds to the C=O stretching range associated with carbonyl/carboxyl groups and has been reported in materials containing annatto [17]. In polymeric materials containing annatto, bands near 1713 cm^{-1}, accompanied by absorptions around 1562 and 1161 cm^{-1}, were also associated with the presence of constituents compatible with bixin [14]. Similarly, in pigments extracted from *Bixa orellana* L. seeds, absorptions in the region near 1717 cm^{-1} were attributed to the dye's carbonyl groups, accompanied by bands near 1608 and 1563 cm^{-1} [18]. In the region of 1608 and 1562–1563 cm^{-1}, the bands can be related to the conjugated system of the organic fraction of annatto. The absorption around 1562 cm^{-1} is usually associated with the C=C stretching of conjugated systems. The band near 1608 cm^{-1} can be assigned to the vibrational region of conjugated organic structures and carbonyl groups in annatto. In PVDF/An composites, these bands are less intense due to the low amount of dopant, but they tend to become more noticeable in samples with higher annatto concentration. From Figure **1**, it can be observed that in the region between 1500 cm^{-1} and 1800 cm^{-1}, PVDF/An 0% shows no vibrational peaks. However, for doped samples in this region, some noise in the results may be related to the addition of annatto. For doped samples, the region around 1254 cm^{-1} can be attributed to a combination of OH angular deformation and C–O stretching, and the region around 1160 cm^{-1}, is related to the stretching of the asymmetric OC=C bond in annatto [17]. The peak at 1160 cm^{-1} overlaps with the PVDF peaks at 1167 cm^{-1} and 1170 cm^{-1}, which correspond to the asymmetric and symmetric CF_2 stretching vibration, respectively [16]. At lower wavenumbers, the doped sample presents a signal near 962 cm^{-1}, which is consistent with sp^2 C–H out-of-plane deformations, while the band near 682 cm^{-1} may be associated with O–H out-of-plane deformation [17]. Taken together, the results indicate that incorporating An into the PVDF matrix preserves vibrational signatures consistent with oxygenated groups, carbonyls, and conjugated systems characteristic of the organic fraction of annatto. Thus, FTIR analysis indicates that PVDF/An films retain the main vibrational structure of PVDF and exhibit discrete yet consistent contributions arising from the presence of the natural dopant. The low relative intensity of these bands in the composites aligns with the concentrations used, given that annatto was incorporated in a small proportion relative to the polymer matrix. Nevertheless, the changes observed in the regions associated with carbonyls, oxygenated groups, and conjugated systems confirm the incorporation of annatto powder into the PVDF films.

From Figure **1**, taking the peaks at 840 cm^{-1} and 763 cm^{-1} and using the Salimi method (Eq. 01), it is possible to determine the relative percentage of β phase (F_β%).

$$(F_\beta\%) = \frac{Abs_\beta}{1.26(Abs_\beta)+Abs_\beta} \qquad \text{Eq. 01}$$

Where Abs_β is the absorption of β phase and Abs_β is the absorption of α phase. The obtained results were approximately 72 %, 75 %, 74 %, 74 %, 73 %, and 74% for PVDF/ An 0 %, 1%, 2 %, 3 %, 4 %, and 5%, respectively. The results did not show a significant variation with An addition and remained practically constant. For optical applications, this result is very

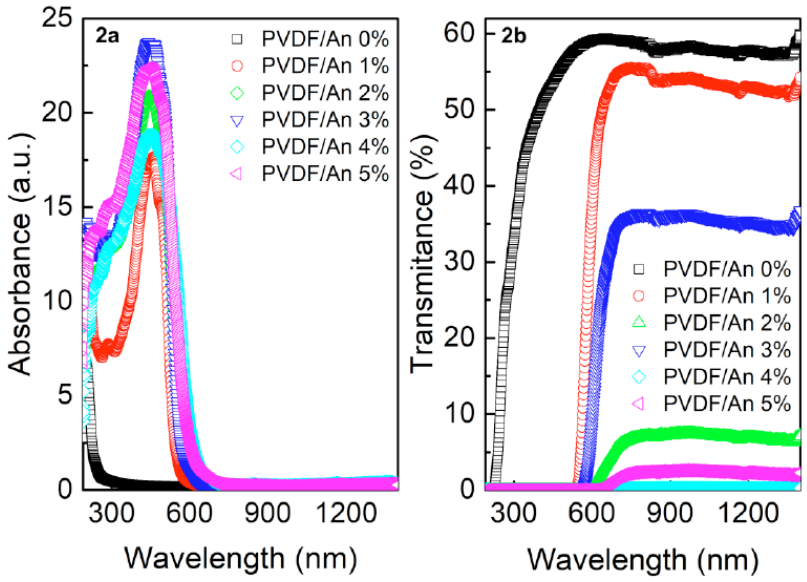

Figure 2: Optical absorbance increases and optical transmittance reduction caused by An addition in the PVDF matrix as a function of An concentration.

important, since an external electric field can control the optical properties in ferroelectric materials [19]. If F_{β}(%) remains constant, it means that the polar phase remains constant, which is indicative that the ferroelectric properties are preserved. If the ferroelectric properties do not change, the control of optical properties is preserved as well. However, further studies are needed to confirm this.

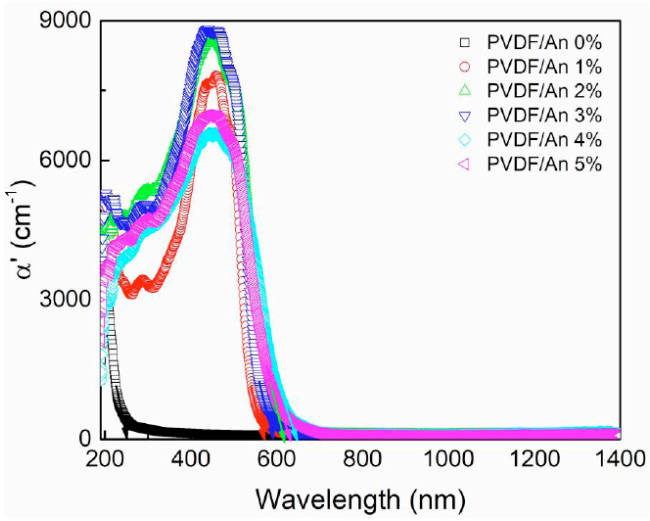

Figure 3: Optical absorption coefficient results and optical absorption edge indication for PVDF/An samples as a function of An content.

Figure **2** displays the experimental results for optical absorbance (A) and transmittance of PVDF/An samples as a function of concentration. In pure PVDF (PVDF/An 0%), the optical absorption observed between 250 nm and 400 nm is attributed to the electronic transition of the fluorocarbons (F–C) [4]. For doped samples, the addition of An broadens the absorption at 505 nm and presents four additional peaks at 287 nm, 432 nm, 458 nm, and 494 nm. These peaks can be attributed to the bixin that presents peaks at 285-293 nm, 429 nm, 457 nm, and 487 nm [20,21]. In Figure **2b**, PVDF/An 0% presents an optical transmittance of almost 60% at 540. For doped samples, the optical transmittance at 540 nm decreases to 0%.

From optical absorbance it is possible to obtain the optical absorption coefficient (α') by Beer-Lambert's formula $\alpha' = 2{,}303\left(\frac{A}{d}\right)$, where d is the thickness of the sample. In Figure **3**, the results for all compositions are displayed. The literature reports that the spectral distribution of the optical absorption coefficient near the band edge can be attributed to the electronic transition between higher occupied molecular orbitals (HOMO) and lower unoccupied molecular orbitals (LUMO) of the molecule, and the absorption edge in isotropic material gives the optical band gap (E_g) [22]. Thus, the absorption edge analysis may provide information on the band gap behavior of the PVDF matrix. Pure PVDF presents an absorption edge at 251 nm and a width at half weight of 30 nm. In a previous work, the authors found absorption edges for pure PVDF at 249 and 255 nm [3, 6]. The absorption edge around 200 nm is related to the semi-crystalline characteristic of PVDF [3]. Doped samples present high optical absorption in the UV and almost the entire visible region of the electromagnetic spectrum. The absorption edge is red-shifted from 251 nm to 645 nm, and the width at half weight is 355 nm. The observed red-shift might be related to a decrease in the optical bandgap.

From optical absorption coefficient is possible to calculate the extinction coefficient by the equation $\kappa = \frac{\alpha'\lambda}{4\pi}$, where λ is the wavelength of incident photon. This parameter is important because it describes the loss of wave energy to the sample (optical loss), and is related to the imaginary part of the complex refractive index by the relation: $\tilde{n} = n + i\kappa$, and n is the refractive index [6]. In Figure **4a**, for PVDF/An 0%, the value found at 200 nm is 0.048 and them decreases as

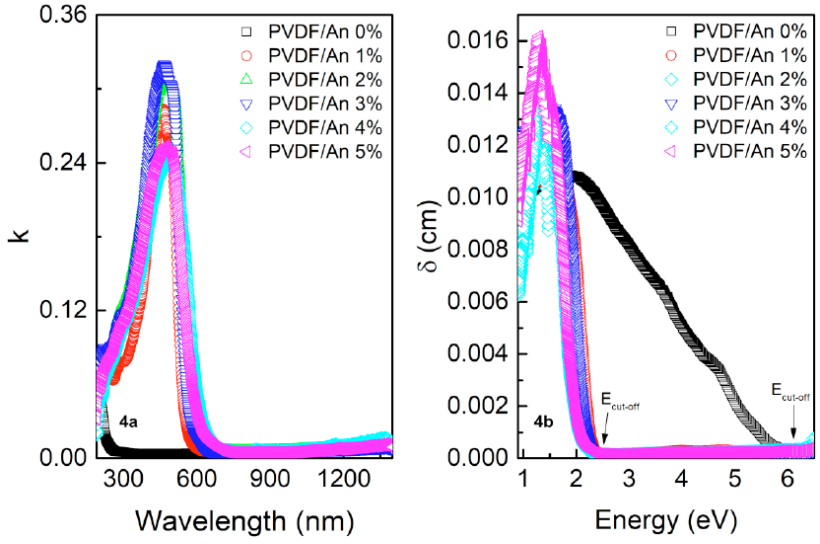

Figure 4: Results of the calculation of Extinction coefficient (**a**) and skin depth (**b**) showing the increase in both parameters for PVDF/An samples as a function of An content.

a function of wavelength up to 430 nm and them increases. On the other hand, PVDF/An 5% presents a value of 0.057 at 200 nm and then shows two peaks at 470 nm and 498 nm with values of 0.253 and 0.248, respectively. This behavior might be related to bixin present in the annatto powder, and the displacement of the observed peaks might be related to the interaction between annatto and the PVDF matrix. For optical applications, as harvesting materials, high values of κ over a broad region of the electromagnetic spectrum are desirable [23]. High values of κ indicate strong photon absorption, which leads to a rapid decay of the electric field amplitude and a small skin depth. Thus, it is important to know the skin depth (δ) or depth-penetration behavior. Skin depth (δ) represents the exponential decay of the incident photon in a medium of finite electrical conductivity, and is related to α' by the following relation $\delta = \frac{1}{\alpha'}$ [3]. In Figure **4b**, the parameter δ for PVDF/An 0% at 1 eV presents a value of 0.01 cm, and after 1.93 eV the values found decreases, reaching the $E_{cut\text{-}off}$ at 6.18 eV. From Figure **4b**, it is possible to see that An addition into the PVDF matrix displaces the $E_{cut\text{-}off}$ to lower energies (2.50 eV) for all doped samples. Since skin depth depends on optical transmittance (T), these results indicate that PVDF loses its transparency with An addition.

For crystalline materials with high optical absorption > 10^4 cm^{-1}, the coefficient α' has a frequency dependence given by

$$\alpha' h\nu = A'(h\nu - E_g)^r \qquad \text{Eq. 1}$$

where E_g is the optical energy gap, and r is the power factor of the transition mode that can assume values of 1/2 and 2 for allowed direct and allowed indirect transitions. The parameter A' is an energy-independent constant called the band tailing parameter. From Eq. 01 it is possible to determine E_g plotting $(\alpha' h\nu)^{\frac{1}{r}}$ against photon energy $(h\nu)$ and taking the extrapolation of linear part up to this intercept the energy axis. PVDF samples may present both direct and indirect bandgap energies. The direct bandgap is related to optical transitions, and the indirect bandgap is important for understanding thermodynamic behavior and electrical conductivity. In Figure **5**, both indirect and direct optical bandgap results are displayed. As can be seen, PVDF/An 0% presents an indirect optical bandgap of 4.93 eV and a direct bandgap of 5.48 eV. In a previous work for pure PVDF, the values found for indirect and direct bandgap were 5.1 eV and 5.6 eV, respectively [6]. Other works report an indirect bandgap of 4.82 eV and 4.96 eV, and values of 5.56 eV and 5.66 eV for direct bandgap [3, 24]. Thus, the obtained results are in agreement with the literature. From Figure **5**, it is also possible to observe that the An addition decreases the indirect bandgap by 1.85 eV and the direct bandgap by 2.15 eV, representing a decrease of approximately 60%. This behavior might be associated with the increase in unstructured bulk defects caused by An addition, and corroborates with the absorption edge results.

Generally, polymers present localized states associated with their bandgaps [22]. These localized states may increase if structural defects increase, causing the Urbach tail to broaden and the energy gap to widen. The Urbach rule can determine the extent of the band tail

$$\alpha' = \alpha_0 \exp\left(\frac{\lambda\nu}{E_U}\right) \qquad \text{Eq. 02}$$

where α_0 is a constant, E_U is the activation energy sometimes called Urbach energy, and represents the width of localized states within the bandgap [25]. The plot of $ln(\alpha')$ against photon energy $(h\nu)$ is used to

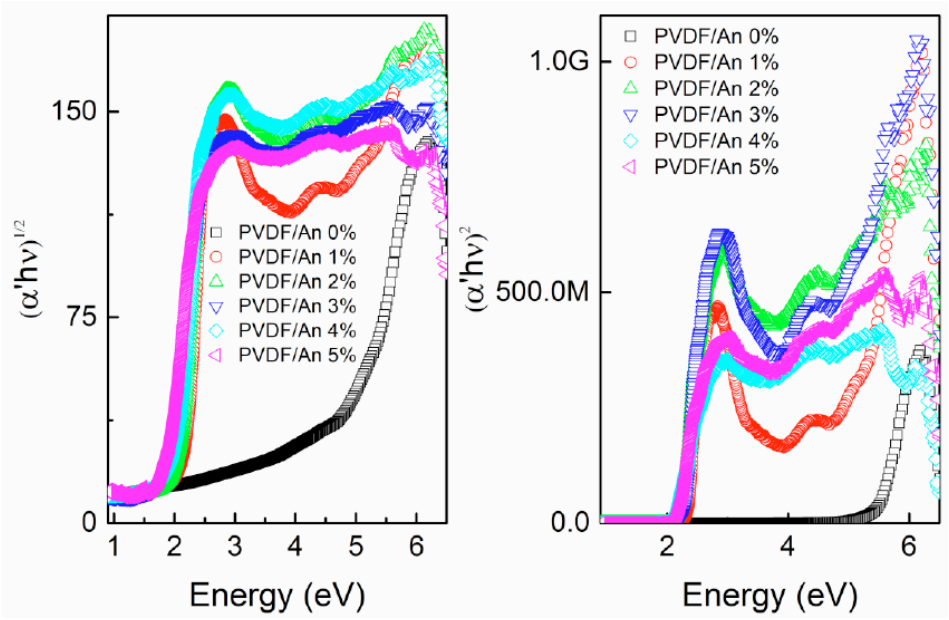

Figure 5: Tauc plot for the obtention of indirect and direct optical bandgap energy for PVDF/An samples as a function of An concentration.

analyze the optical absorption near to the band edge. The slopes of its linear part are inversely proportional to the E_U. Thus, an increase in the slope indicates a decrease in E_U, suggesting an increase in localized states within the material and an increase in structural disorder [26]. The results for Urbach energy and optical bandgap are plotted in Figure **6**. As can be seen, the incorporation of annatto into the PVDF matrix decreases E_U from 0.598 eV to 0.147 eV as the An content increases. This behavior might be associated with defects induced in the polymeric matrix by dopant. These induced defects increase structural disorder, which in turn increases the density of localized states, narrowing the energy barrier for electronic transitions and reducing E_g [26]. This reduction in the bandgap energy means PVDF/An composites require less energy for optical absorption, justifying the redshift observed in the optical absorption edge. This work shows that the optical response of PVDF/An is governed by a highly interconnected network of electronic and structural parameters. The addition of filler increases structural disorder and structural defects, thereby decreasing the optical bandgap energy and allowing PVDF/An to absorb lower photon energy. This absorption increases the extinction coefficient near the band edge and reduces the penetration depth.

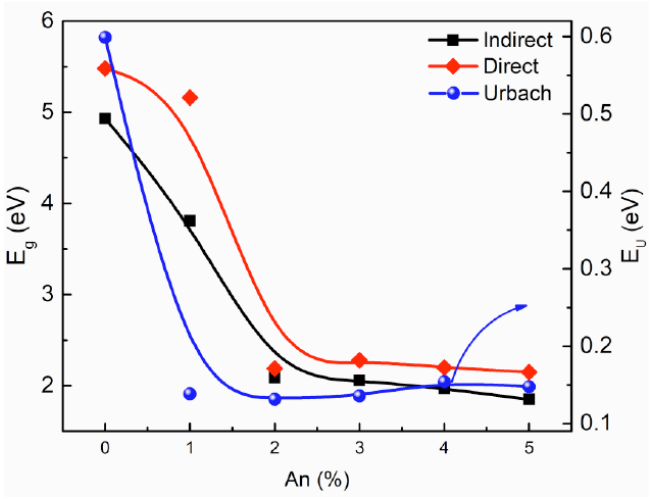

Figure 6: Comparison among the results of Indirect and direct optical bandgap and Urbach energy results for PVDF/An samples as a function of An concentration.

CONCLUSION

In this work, annatto powder was used as a dopant for PVDF polymer as a function of concentration. FT-IR measurements showed that An addition in the polymeric matrix did not change the relative percentage of the β phase. From UV-Vis measurements, it was observed that An addition broadened absorption at 505 nm, presenting four additional peaks attributed to bixin. PVDF/An 0% presents an optical transmittance of 60% at 540 nm. For other compositions in this region, the transmittance drops to 0%. For PVDF/An 0%, the optical absorption coefficient presents an absorption edge at 251nm. However, for other compositions, the absorption edge is shifted to 645 nm. The addition of An to the PVDF matrix increases the extinction coefficient, presenting two peaks at 470 nm and 498 nm, associated with the bixin. This indicates that electromagnetic waves lose more energy in this region than in others. From the skin depth, it was observed that the $E_{cut\text{-}off}$ decreased from 6.18 eV to 2.50 eV, indicating that PVDF loses its transparency. The results also show a decrease in bandgap decrease as a function of An content, which is consistent with the absorption edge results. The decrease in bandgap is associated with an increase in structural defects, which increases the density of localized states. The localized states are related to the Urbach energy, and a decrease in this energy indicates increased structural disorder. The obtained results showed that E_U decreases with An addition, indicating an increase in structural defects and a decrease in the bandgap. Finally, the reduction in optical transmittance, the redshift of the absorption edge, the increase in the extinction coefficient, the reduction in the $E_{cut\text{-}off}$, and the observed reduction in bandgap and Urbach energy indicate that PVDF/An samples are potential candidates for optical and photonic applications and for UV protection.

AUTORS' CONTRIBUTION

T. S. Silva, Sample preparation, Investigation, Writing - original draft; L. G. N. Muniz: Sample preparation, Investigation; E. S. S. Rodrigues: Sample preparation, Investigation; E.A. Falcao: Project administration, Supervision, Conceptualization, Methodology, Resources, Investigation, Visualization, Formal analysis, Writing - original draft, Review & editing.

ACKNOWLEDGEMENTS

The authors are grateful to the Brazilian Agencies: CAPES, CNPq (process 483683/2010-8), FINEP (contract 04.13.0448.00/2013), and FUNDECT (process 83/026.883/2024) for the financial support of this work.

DECLARATION OF CONFLICTING INTEREST

The authors of this work declare that there is no conflict of interest in the submission of this manuscript, and it was approved by all authors for publication.

REFERENCES

[1] X. Cai, T. Lei, D. Sun, *et al.*, A Critical Analysis of the α, β and γ Phases in Poly(vinylidene fluoride) Using FTIR. RSC

Advances 7 (2017) 15382-15389.
https://doi.org/10.1039/C7RA01267E

[2] E. A. Falcao, A. C. Silva, R. Guo, *et al*., Synthesis and Structural Characterization of PVDF-Based Lead-Free Ceramic Composites. Ferroelectrics, v. 611, n. 1, p. 129-137, 2023.
https://doi.org/10.1080/00150193.2023.2201776

[3] E. A. Falcao, L. W. Aguiar, R. Guo, A. S., Optical Absorption of Nd_2O_3-Doped Polyvinylidene Fluoride films. Mat. Chem. and Phys. 258 (2021) 123904, 2021.
https://doi.org/10.1016/j.matchemphys.2020.123904

[4] L. W. Aguiar, E. R. Botero, E. A. Falcao, *et al*., Study of the Changes in the Polar Phase and Optical Properties of Poly(Vinylidene Fluoride) Matrix by Neodymium Compound Additon. Mat. Today. Comm. 25 (2020) 101274.
https://doi.org/10.1016/j.mtcomm.2020.101274

[5] E. A. Falcao, L. W. Aguiar, C. T. Carvalho, *et al*., Ultraviolet Optical Absorption Enhancement and Bandgap Decrease in PVDF Matrix Promoted by the Addition of Nd/trans-3,4-(Methylenedioxy)Cinnamic Complex. Materials Letters, v. 367, 136647, 2024.
https://doi.org/10.1016/j.matlet.2024.136647

[6] E. A. Falcão, T. Silva, E. S. S. Rodrigues, S. M. Martelli, Enhancement of Optical Absorption and Bandgap Decrease of PVDF/Curcuma longa Linn Composites: UV-Vis Technique. J. of Comp. and Biod. Poly., 13 (2025) 119-125, 2025.
https://doi.org/10.12974/2311-8717.2025.13.09

[7] S. Paramadhas, P. Selvi, B. Shridar *et al*., Optimization and Extraction of Annatto Pigments Obtained from Bixa Orellana L. Using Supercritical Fluid Extraction, Microchem. Jour. 206 (2024) 111494.
https://doi.org/10.1016/j.microc.2024.111494

[8] B. J. Demczuk, R. H. Ribani, Atualidades Sobre a Química e a Utilização do Urucum (Bixa orellana L.). Ver. Bras. de Pesq. em Alim. 6 [1] (2015) 37-50.
https://doi.org/10.14685/rebrapa.v6i1.144

[9] C. E. R. Garcia, V. J. Bolognesi, J. F. G. Dias, *et al*., Carotenoids Bixin and Norbixin from Annatto (Bixa orellana L.) as Antioxidants in Meat Products. Ciên. Rural 42 [8] (2012) 1510-1517.
https://doi.org/10.1590/S0103-84782012000800029

[10] Shahid-ul-Islam, L. J. Rather, F. Mohammad, Phytochemistry, Biological Activities and Potential of Annatto in Natural Colorant Production for Industrial Applications – A review, J. of Adv. Res 7 [3] (2016) 499-514.
https://doi.org/10.1016/j.jare.2015.11.002

[11] M. G. Silva, A. L. Garcia, E. S. Brito, *et al*., The annatto carotenoids and the norbixin absorption coefficient. Revista do Instituto Adolfo Lutz, São Paulo, v. 77, e1737, 2018.
https://doi.org/10.53393/rial.2018.v77.34173

[12] E. Aluko, Ethanol-Based Extraction of Annatto (Bixa orellana L.) and Characterization of the Bixin and Norbixin. ACS Omega 9 (2024) 18273-18277.
https://doi.org/10.1021/acsomega.3c10120

[13] S. Zongo, A. P. Kerasidou, B. Sone, *et al*., Nonlinear optical properties of poly(methyl methacrylate) thin films doped with Bixa orellana dye. App. Surf. Sci. 340 (2015) 72-77.
https://doi.org/10.1016/j.apsusc.2015.02.161

[14] C. S. Pagnan, A. C. Mottin, R. L. Oréfice, *et al*., Annatto-colored Poly(3-hydroxybutyrate): A Comprehensive Study on Photodegradation. J Polym Environ 26 (2018) 1169-1178.
https://doi.org/10.1007/s10924-017-1026-1

[15] L. P. Fontinele, R. C. Sousa, V. G. F. Viana, *et al*., Norbixin Extracted from Urucum (Bixa orellana L.) for the Formation of Conductive Composites with Potential Applications in Electrochemical Sensors. Surfaces and Interfaces 13 (2018) 92-100.
https://doi.org/10.1016/j.surfin.2018.08.002

[16] A. M. Ismail, R. Ramadan, M. M. El‐Masry, The Role of Nanoparticles Inclusion in Monitoring the Physical Properties of PVDF, J. of the Aust. Cer. Soc. [59] (2023) 333–341.
https://doi.org/10.1007/s41779-023-00836-4

[17] D. S. Corrêa, L. F. Lyra, F. M. Broca, A. M. Barbosa, e K. K. Sakane, "Use of Infrared Spectroscopic Techniques (FTIR-UATR), Coupled with Multivariate Statistical Analyses, in the Quality Analysis of Food Colorings Containing Urucum", Rev. Univap 30 [66] (2024).

[18] COSTA, Charllyton Luis S. da; CHAVES, Mariana H. Extraction of Pigments From Seeds of Bixa Orellana L.: An Alternative for Experimental Courses in Organic Chemistry. Quim. Nova 28 [1] (2005) 149-152.
https://doi.org/10.1590/S0100-40422005000100026

[19] E. A. Falcao, J. A. Eiras, D. Garcia, *et al*., Electrical Field Dependence of Thermo-Optical Parameters in Transparent Lead Lanthanum Zirconated Titanate Ceramic: Thermal Lens Measurements, J. Appl. Phys. 110 (2011) 123517.
https://doi.org/10.1063/1.3671425

[20] W. Rahmalia, J. F. Fabrea, T. Usman, Z. Mouloungui, Aprotic solvents effect on the UV–visible absorption spectra of bixin, Spec. Acta Part A: Mole. and Biom. Spect. 131 (2014) 455-460.
https://doi.org/10.1016/j.saa.2014.03.119

[21] D. T. Bueno, A. F. Leitzke, R. L Crizel, at all., Characterization of Bixin by UV-Visible Spectroscopy and HPLC, and Its Application as Latent Fingermark Developer, Analy. 5 (2024) 107-118.
https://doi.org/10.3390/analytica5010007

[22] E. A. Gaml, Hajer Abusnina and N. A. El-Ghamaz, Absorption, dispersion, and emission characteristics of novel Chitosan blends thin films tuned by UV-Ozone, Sci. Rep. (2026) 16:9680.
https://doi.org/10.1038/s41598-026-40385-x

[23] H. Li, C. Cui, X. Xu, *et al*., A Review of Characterization of Perovskite Film in Solar Cells by Spectroscopic Ellipsometry, Sol. Ener. 212 (2020) 48–61.
https://doi.org/10.1016/j.solener.2020.10.066

[24] A.P. Indolia, M.S. Gaur, Optical properties of solution grown PVDF-ZnO nanocomposite thin films, J. Polym. Res. 20 (2013) 43-51.
https://doi.org/10.1007/s10965-012-0043-y

[25] E. A. Davis & N. F. Mott, Conduction in Non-crystalline Systems V. Conductivity, Optical Absorption and Photoconductivity in Amorphous Semiconductors, Phil. Mag. 22 [179] (1970) 0903-0922.
https://doi.org/10.1080/14786437008221061

[26] D. M. Mamand, D. S. Muhammad, S. B. Aziz, Peshawa O. Hama, B. A. Al-Asbahi, A. A. A. Ahmed, J. Hassan, Enhanced Optical Properties of Chitosan Polymer Doped with Orange Peel Dye Investigated via UV–Vis and FTIR Analysis. Sci Rep15, 3232 (2025).
https://doi.org/10.1038/s41598-025-87425-6

https://doi.org/10.12974/2311-8717.2026.14.08